
Predicting time-varying distributions with limited training data

Connie Kou

School of Computing, National University of Singapore
Bioinformatics Institute, A*STAR, Singapore
koukl@comp.nus.edu.sg

Hwee Kuan Lee

School of Computing, National University of Singapore
Bioinformatics Institute, A*STAR, Singapore
leehk@bii.a-star.edu.sg

Teck Khim Ng

School of Computing, National University of Singapore
ngtk@comp.nus.edu.sg

Jorge Sanz

School of Business, National University of Singapore
School of Computing, National University of Singapore
jorges@nus.edu.sg

Abstract

In the task of distribution-to-distribution regression, a recently proposed model, distribution regression network (DRN) (Kou et al., 2018) has shown superior performance compared to conventional neural networks while using much fewer parameters. The key novelty of DRN is that it encodes an entire distribution in each network node, and this compact representation allows DRN to achieve better accuracies than conventional neural networks. However, the experiments in Kou et al. (2018) focused mainly on non-time series data and there is no systematic study on how DRN performs with limited annotated data. The ability to train well with limited training data is an important feature in the current supervised training paradigm. In this paper, we evaluate DRN for the new task of performing forward prediction on time sequences of probability distributions. We also perform extensive studies on how the test performance varies with the size of training data since for time series, the number of data may be limited given the seasonality of the data. In our experiments, we show that DRN requires two to five times fewer training data than neural networks to achieve similar prediction accuracies. However, DRN is a feedforward network and does not explicitly model time dependencies. Hence we propose a new recurrent architecture for DRN, named recurrent distribution regression network (RDRN). In our experiments involving prediction on sequences of distributions, RDRN and DRN outperform neural network models, with RDRN achieving similar or better accuracies than DRN.

Deep neural networks have achieved state-of-the-art results in many tasks by designing the network architecture according to the data type. For instance, the convolutional neural network (CNN) uses local filters to capture the features in an image and max pooling to reduce the image feature size. By

using a series of convolution and max pooling layers, CNN extracts the semantic meaning of the image. The recurrent architecture of recurrent neural networks (RNN) when unrolled, presents a shared weight structure which is designed to model time dependencies in a data sequence. However, among the major network architectures, there is no architecture suitable for regression on function spaces. In particular, neural networks are unable to represent function inputs compactly. Since each node encodes only a real value, a function has to be decomposed to smaller parts that are represented by separate nodes. When the function has been decomposed into separate nodes, the notion of function is no longer captured explicitly. A recently proposed network, distribution regression network (DRN) (Kou et al., 2018), has solved this problem for the task of distribution-to-distribution regression. DRN uses a novel representation of encoding an entire distribution in a single node, allowing DRN to use more compact models that achieve superior performance. It has been shown that DRN can achieve better accuracies with 500 times fewer parameters compared to the multilayer perceptron (MLP).

However, the experiments in Kou et al. (2018) focused mainly on non-time series data and it is also not known how DRN performs with limited training data. In this paper, we further investigate the strengths of DRN for the task of performing forward prediction on time sequences of probability distributions, which has many applications from stock market prediction (Cenesizoglu & Timmermann, 2008) to weather forecasting (Palmer, 2000). We also perform detailed studies on how the test performance varies with the size of training data. For time series data, it is important to be able to use fewer training data given the seasonality of the data. For instance, for prediction tasks involving stock and commodity markets, the valid training data may have a short time window due to changing market conditions (Kaastra & Boyd, 1996). Through our experiments, we find that DRN consistently outperforms neural networks, requiring two to five times fewer training data to achieve similar generalization performance. As the number of training data decreases, DRN’s test accuracy remains high whereas the neural network models saw more drastic decrease in test accuracy.

Despite the strengths of DRN, it is a feedforward network and hence it does not explicitly model time dependencies in a sequence of distributions. To that end, we propose a recurrent extension of DRN, named the recurrent distribution regression network (RDRN). In the hidden states of RDRN, each node represents a distribution, thus containing much richer information while using fewer weights compared to the real-valued hidden states in recurrent neural networks. In comparison to DRN, the shared weights architecture in RDRN is designed to capture time dependencies better. In our experiments involving forward prediction on sequences of distributions, RDRN and DRN outperform neural network models, with RDRN achieving similar or better accuracies than DRN.

1 Related Work

Performing forward prediction on time-varying distributions has many important applications. Many real-world systems are driven by stochastic processes. For such systems, the Fokker-Planck equation (Riskin, 1996) has been used to model a time-varying distribution, with applications in astrophysics (Noble & Wheatland, 2011), biological physics (Guérin et al., 2011), animal population studies (Butler & King, 2004) and weather forecasting (Palmer, 2000). In these applications, it is very useful to predict the future state of the distribution. For example, the Ornstein-Uhlenbeck process, which is a specific case of the Fokker-Planck equation, has been used to model and predict commodity prices (Schwartz & Smith, 2000). Extrapolating a time-varying distribution into the future has also been used for predictive domain adaptation, where a classifier is trained on data distribution which drifts over time (Lampert, 2015).

Various machine learning methods have been proposed for distribution data, ranging from distribution-to-real regression (Póczos et al., 2013; Oliva et al., 2014) to distribution-to-distribution regression (Oliva et al., 2015, 2013). The Triple-Basis Estimator (3BE) has been proposed for the task of function-to-function regression. It uses basis representations of functions and learns a mapping from Random Kitchen Sink basis features (Oliva et al., 2015). The authors have applied 3BE for distribution regression, showing improved accuracy and speed compared to an instance-based learning method (Oliva et al., 2013). More recently, Kou et al. (2018) proposed the distribution regression network which extends the neural network representation such that an entire distribution is encoded in a single node. With this compact representation, DRN showed better accuracies while using much fewer parameters than conventional neural networks and 3BE (Oliva et al., 2015).

The above methods are for general distribution regression. For predicting the future state of a time-varying distribution, it is important to model the time dependencies in the distribution sequence. Lampert (2015) proposed the Extrapolating the Distribution Dynamics (EDD) method which predicts the future state of a time-varying distribution given a sequence of samples from previous time steps. EDD uses the reproducing kernel Hilbert space (RKHS) embedding of distributions and learns a linear mapping to model the dynamics of how the distribution evolves between adjacent time steps. EDD is shown to work for a few variants of synthetic data, but the performance deteriorates for tasks where the dynamics is non-linear. Since the regression is performed with just one input time step, it is unclear how EDD can be extended for more complex trajectories that require multiple time steps of history. Another limitation is that the EDD can only learn a single trajectory of the distribution and not from multiple trajectories.

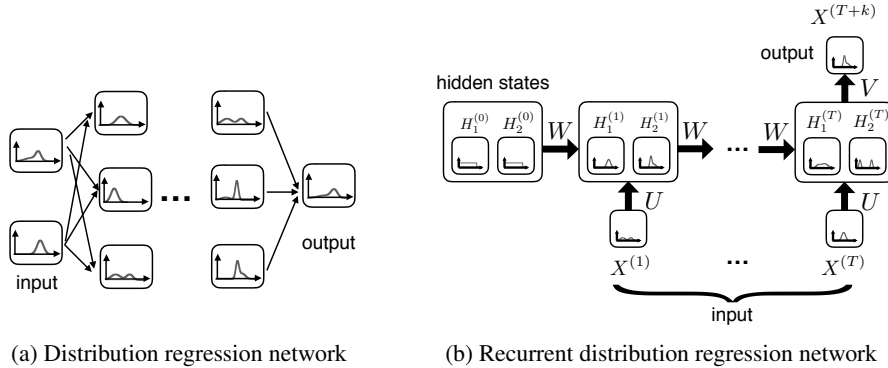


Figure 1: (a) A schematic of distribution regression network (DRN) which performs distribution regression by encoding each node with an entire distribution. (b) An example network for recurrent distribution regression network (RDRN) which takes in T time steps of distributions to predict the distribution at $T + k$. The arrows represent fully-connected weights. The input-hidden weights U and the hidden-hidden weights W are shared across time steps. V is the weights between the final hidden state and the output distribution. The hidden states at $t = 0$ are initialized as uniform distributions.

2 Recurrent distribution regression network (RDRN)

2.1 Time-series distribution regression

We address the task of forward prediction from a time-varying distribution: Given a series of distributions with T equally-spaced time steps, $X^{(1)}, X^{(2)}, \dots, X^{(T)}$, we want to predict $X^{(T+k)}$, ie. the distribution at k time steps later. We assume the distributions to be univariate. The input at each time step may consist of more than one distribution. In this case, the input distribution sequence is denoted as $(X_1^{(1)}, \dots, X_n^{(1)}), \dots, (X_1^{(T)}, \dots, X_n^{(T)})$, where there are n data distributions per time step.

Performing prediction on distribution sequences requires both compact distribution representations and modeling of time dependencies. While the recurrent neural network works well for time series data, it has no efficient representation for distributions. As for DRN, although it has a compact representation for distributions, the feedforward architecture does not explicitly capture the time dependencies in the distribution sequence. Hence, we propose our recurrent distribution regression network (RDRN) which is a recurrent extension of DRN.

2.2 Background: distribution regression network (DRN)

Neural network models work well if the network architecture is designed according to the data type. Convolutional neural networks are suited for image data as they employ convolution to capture local features from neighboring image pixels. Such important data domain knowledge is not built in the fully-connected multilayer perceptron. For analysis of distributions, there are no conventional neural network architectures like what CNN does for images. To that end, Kou et al. (2018) proposed

the distribution regression network (DRN) for the task of distribution-to-distribution regression. To cater to distribution data, DRN has two main innovations: 1) each network node encodes an entire distribution and 2) the forward propagation is specially designed for propagating distributions, with a form inspired by statistical physics (Katsura, 1962; Lee et al., 2002, 2003; Wu, 1982).

We give a brief description of DRN following the notations of Kou et al. (2018). Figure 1a illustrates the propagation in DRN. Similar to MLP, DRN consists of multiple fully-connected layers connecting the data input to the output in a feedforward manner, where each connection has a real-valued weight. The novelty of DRN is that each node in the network encodes a univariate probability distribution. The distribution at each node is computed using the distributions of the incoming nodes, the weights and the bias parameters. Let $P_k^{(l)}$ represent the probability density function (pdf) of the k^{th} node in the l^{th} layer where $P_k^{(l)}(s_k^{(l)})$ is the density of the distribution when the node variable is $s_k^{(l)}$. The unnormalized distribution $\tilde{P}_k^{(l)}$ is computed by marginalizing over the product of the unnormalized conditional probability $\tilde{Q}(s_k^{(l)} | s_1^{(l-1)}, \dots, s_n^{(l-1)})$ and the incoming probabilities.

$$\tilde{P}_k^{(l)}(s_k^{(l)}) = \int_{s_1^{(l-1)}} \dots \int_{s_n^{(l-1)}} \tilde{Q}(s_k^{(l)} | s_1^{(l-1)}, \dots, s_n^{(l-1)}) P_1^{(l-1)}(s_1^{(l-1)}) \dots P_n^{(l-1)}(s_n^{(l-1)}) ds_1^{(l-1)} \dots ds_n^{(l-1)} \quad (1)$$

$$\tilde{Q}(s_k^{(l)} | s_1^{(l-1)}, \dots, s_n^{(l-1)}) = e^{-E(s_k^{(l)} | s_1^{(l-1)}, \dots, s_n^{(l-1)})} \quad (2)$$

The unnormalized conditional probability has the form of the Boltzmann distribution, where E is the energy for a given set of node variables,

$$E(s_k^{(l)} | s_1^{(l-1)}, \dots, s_n^{(l-1)}) = \sum_i^n w_{ki}^{(l)} \left(\frac{s_k^{(l)} - s_i^{(l-1)}}{\Delta} \right)^2 + b_{q,k}^{(l)} \left(\frac{s_k^{(l)} - \lambda_{q,k}^{(l)}}{\Delta} \right)^2 + b_{a,k}^{(l)} \left| \frac{s_k^{(l)} - \lambda_{a,k}^{(l)}}{\Delta} \right|, \quad (3)$$

where $w_{ki}^{(l)}$ is the weight connecting the i^{th} node in layer $l-1$ to the k^{th} node in layer l . $b_{q,k}^{(l)}$ and $b_{a,k}^{(l)}$ are the quadratic and absolute bias terms acting on positions $\lambda_{q,k}^{(l)}$ and $\lambda_{a,k}^{(l)}$ respectively. Δ is the support length of the distribution. After obtaining the unnormalized probability, the distribution from Eq. (1) is normalized. Forward propagation is performed layer-wise to obtain the output prediction.

The DRN propagation model, with the Boltzmann distribution and the energy function, is motivated by work on spin models in statistical physics (Katsura, 1962; Lee et al., 2002, 2003; Wu, 1982). With such a propagation method, DRN exhibits useful propagation properties such as peak spreading, peak shifting, peak splitting and the identity mapping, with just a few network parameters (Kou et al., 2018). Due to space constraints, we refer the readers to Kou et al. (2018) for a more detailed description.

2.3 Extension to recurrent architecture

Since DRN is a feedforward network, it does not explicitly capture the time dependencies in distribution sequences. In this work, we introduce our recurrent distribution regression network (RDRN) which is a recurrent extension of DRN. The input data is a distribution sequence as described in Section 2.1. Figure 1b shows an example network for RDRN, where the network takes in T time steps of distributions to predict the distribution at $T+k$. The hidden state at each time step may consist of multiple distributions. The arrows represent fully-connected weights. The input-hidden weights U and the hidden-hidden weights W are shared across the time steps. V represents the weights between the final hidden state and the output distribution. The bias parameters for the hidden state nodes are also shared across the time steps. The hidden state distributions at $t=0$ represents the ‘memory’ of all past time steps before the first input and can be initialized with any prior information. In our experiments, we initialize the $t=0$ hidden states as uniform distributions as we assume no prior information is known.

We formalize the propagation for the general case where there can be multiple distributions for each time step in the data input layer and the hidden layer. Let n and m be the number of distributions per time step in the data layer and hidden layers respectively. Propagation starts from $t=1$ and performed through the time steps to obtain the hidden state distributions. $X_i^{(t)}(r_i^{(t)})$ represents the input data distribution at node i and time step t , when the node variable is $r_i^{(t)}$. $H_k^{(t)}(s_k^{(t)})$ represents the density of the pdf of the k^{th} hidden node at time step t when the node variable is $s_k^{(t)}$. $\tilde{H}_k^{(t)}(s_k^{(t)})$ represents the unnormalized form. The hidden state distributions at each time step is computed from the hidden state distributions from the previous time step and the input data distribution from the current time step.

$$\tilde{H}_k^{(t)}(s_k^{(t)}) = \int_{r_1^{(t)}, \dots, r_n^{(t)}, s_1^{(t-1)}, \dots, s_m^{(t-1)}} \tilde{Q}(s_k^{(t)} | r_1^{(t)}, \dots, s_1^{(t-1)}, \dots) X_1^{(t)}(r_1^{(t)}) \dots X_n^{(t)}(r_n^{(t)}) H_1^{(t-1)}(s_1^{(t-1)}) \dots H_m^{(t-1)}(s_m^{(t-1)}) dr_1^{(t)} \dots dr_n^{(t)} ds_1^{(t-1)} \dots ds_m^{(t-1)} \quad (4)$$

$$\tilde{Q}(s_k^{(t)} | r_1^{(t)}, \dots, s_1^{(t-1)}, \dots) = e^{-E(s_k^{(t)} | r_1^{(t)}, \dots, s_1^{(t-1)}, \dots)} \quad (5)$$

The energy function is similar to the one in DRN and is given by

$$E(s_k^{(t)} | r_1^{(t)}, \dots, s_1^{(t-1)}, \dots) = \sum_i^n u_{ki} \left(\frac{s_k^{(t)} - r_i^{(t)}}{\Delta} \right)^2 + \sum_j^m w_{kj} \left(\frac{s_k^{(t)} - s_j^{(t-1)}}{\Delta} \right)^2 + b_{q,k} \left(\frac{s_k^{(t)} - \lambda_{q,k}}{\Delta} \right)^2 + b_{a,k} \left| \frac{s_k^{(t)} - \lambda_{a,k}}{\Delta} \right|, \quad (6)$$

where for each time step, u_{ki} is the weight connecting the i^{th} input distribution to the k^{th} hidden node. Similarly, for the hidden-hidden connections, w_{kj} is the weight connecting the j^{th} hidden node in the previous time step to the k^{th} hidden node in the current time step. As in DRN, the hidden node distributions are normalized before propagating to the next time step. At the final time step, the output distribution is computed from the hidden state distributions, through the weight vector V and bias parameters at the output node.

2.4 Network cost and optimization

Following Kou et al. (2018), the cost function for the forward prediction task is measured by the Jensen-Shannon (JS) divergence (Lin, 1991) between the label ($X^{(T+k)}$) and predicted ($\hat{X}^{(T+k)}$) output distributions, denoted here as $D_{JS}(X^{(T+k)} || \hat{X}^{(T+k)})$. The network cost function is the average D_{JS} over all training data. Optimization is performed by backpropagation through time. We adopt the same parameter initialization method as Kou et al. (2018), where the network weights and bias are randomly initialized following a uniform distribution and the bias positions are uniformly sampled from the support length of the data distribution. The integrals in Eq. (4) are performed numerically. Each continuous distribution density function is discretized by partitioning into q bins, resulting in a discrete probability mass function (ie. a q -dimensional vector that sums to one).

3 Experiments

We conducted experiments on four datasets which involve prediction of time-varying distributions. To evaluate the effectiveness of the recurrent structure in RDRN, we compare with DRN where the input distributions for all time steps are concatenated at the input layer. We also compare with conventional neural network architectures and other distribution regression methods. The benchmark methods are DRN, RNN, MLP and Triple-Basis Estimator (3BE) (Oliva et al., 2015). For the third dataset, we also compare with Extrapolating the Distribution Dynamics (EDD) (Lampert, 2015) as the data involves only a single trajectory of distribution. Among these methods, RNN and EDD are designed to take in the inputs sequentially over time while for the rest the inputs from all T time steps are concatenated. For a fair comparison, for all methods, we conduct thorough cross-validation

for hyperparameter tuning and to select the best network architectures (for RDRN, DRN, RNN and MLP) or the best number of model parameters (for 3BE). In other words, we perform comparisons with all methods at their optimal performance. In A, we include details of the model architectures and experimental setup.

3.1 Benchmark methods

3.1.1 Distribution regression network (DRN)

Since DRN is a feedforward network, the distributions for all input time steps are concatenated and fed in together. The architecture consists of fully-connected layers, where each node encodes an entire distribution. As in Kou et al. (2018), DRN is optimized using JS divergence. We have also tried optimizing using the mean squared error between the predicted and output distributions but attained similar performance.

3.1.2 Recurrent neural network (RNN)

At each time step, the distribution is discretized into bins and represented by separate input nodes. The RNN architecture consists of a layer of hidden states, where the number of nodes is chosen by cross validation. The input-hidden and hidden-hidden weights are shared across time steps. The final hidden state is transformed by the hidden-output weights and processed by a softmax layer to obtain the output distribution. The cost function is the mean squared error between the predicted and output distributions. We also tried using JS divergence but the performance was similar.

3.1.3 Multilayer perceptron (MLP)

The input layer consists of the input distributions for all time steps and each distribution is discretized into bins that are represented by separate nodes. Hence, for T input time steps and discretization size of q , there will be $T \times q$ input nodes in MLP. MLP consists of fully-connected layers and a final softmax layer, and is optimized with the mean squared error. We have also tried using JS divergence but the performance was similar.

3.1.4 Triple-Basis Estimator (3BE)

For 3BE, each distribution is represented by its sinusoidal basis coefficients. The optimal number of basis coefficients and Random Kitchen Sink basis functions are found using cross validation.

3.1.5 Extrapolating the Distribution Dynamics (EDD)

Since EDD learns from a single trajectory of distribution, it is unsuitable for most of the datasets. We performed EDD for the CarEvolution dataset which has only a single distribution trajectory. For the RKHS embedding of the distributions, we use the radial basis function kernel, following Lampert (2015).

3.2 Shifting Gaussian

For the first experiment, we chose a dataset where the output distribution has to be predicted from multiple time steps of past distributions. Specifically, we track a Gaussian distribution whose mean varies in the range $[0.2, 0.8]$ sinusoidally over time while the variance is kept constant at 0.01. We use this dataset to test the abilities of the models to predict the evolution of unimodal, constant variance distributions with non-linear shifts in the mean values.

Given a few consecutive input distributions taken from time steps spaced $\Delta t = 0.2$ apart, we predict the next time step distribution. Figure 2a illustrates how the mean changes over time. Due to the non-linear variation of the mean over time, it is apparent that we require more than one time step of past distributions to predict the future distribution. For instance, at two different time points, the distribution means can be the same, but one has increasing mean while the other has a decreasing mean. To create the dataset, for each data we randomly sample the first time step from $[0, 2\pi]$. The distributions are truncated with support of $[0, 1]$ and discretized with $q=100$ bins. We found that for all methods, a history length of 3 time steps is optimal. Following Oliva et al. (2014) the regression performance is measured by the L_2 loss, where lower L_2 loss is favorable.

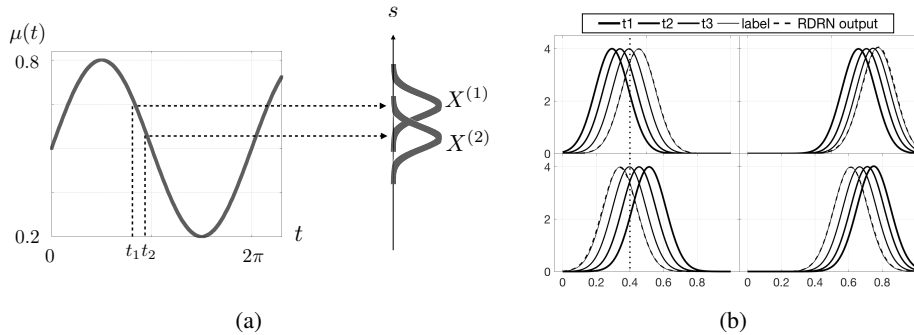


Figure 2: (a) Shifting Gaussian dataset: The mean of the Gaussian distribution varies sinusoidally with time, hence forward prediction requires more than one time step of past distributions. (b) RDRN’s prediction for four test data for the shifting Gaussian dataset shows a good fit with the labeled output. The top and bottom left data have the same mean at $t = 3$, but are moving in opposite directions, showing that more than one input time steps are required for this task.

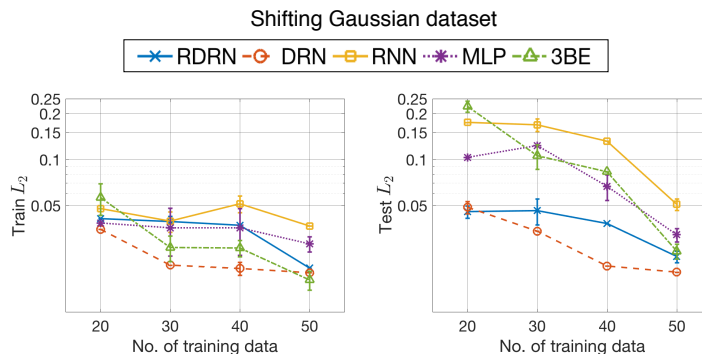


Figure 3: The train and test performance of all methods for the shifting Gaussian dataset as number of training data varies. The accuracies of RDRN and DRN remain high as number of training data decreases, whereas RNN, MLP and 3BE saw more drastic decrease in accuracy. Errorbars are smaller than the size of the symbols when not shown. Best viewed in color.

The plots in Figure 3 show the train and test L_2 loss as the number of training data varies. Across the varying training sizes, RDRN and DRN outperform the other methods (RNN, MLP, 3BE), except at training size of 50, where 3BE’s test performance catches up with RDRN and DRN. As training size decreases, RNN, MLP and 3BE show larger decrease in test performance. DRN performs better than RDRN, except at the smallest training size of 20 where there is no significant difference. Table 1 shows the regression results for the training size of 20, and we note RDRN and DRN use much fewer parameters than RNN, MLP and 3BE. Overall, RDRN and DRN require at least two times fewer training data than the other methods to achieve similar test accuracies, showing that it is important to have efficient representations for distribution data. Note that we have conducted thorough hyperparameter tuning so the network architectures used are optimal under cross-validation, even if it results in a gap between the train and test accuracies.

Figure 2b shows four test data, where the input distributions at $t=1, 2, 3$ are shown, along with the label output for $t=4$ and RDRN’s prediction (trained with 20 data). We observe good fit for the predictions. Additionally, the top and bottom left data shows that two data can have the same mean at $t=3$, but are moving in opposite directions. Hence, to predict the next distribution at $t=4$, multiple time steps in history are required as input and the model has to determine the direction of movement from the history of distributions. The output results show that RDRN is able to model time dependencies in the distribution sequence and infer non-linear variation of the distribution mean.

	Shifting Gaussian (20 training data)			Climate Model (100 training data)		
	Test $L_2(10^{-2})$	T	N_p	Test $L_2(10^{-2})$	T	N_p
RDRN	4.55(0.42)	3	59	11.98(0.13)	5	59
DRN	4.90(0.46)	3	224	12.27(0.34)	3	44
RNN	17.50(0.89)	3	2210	13.29(0.59)	5	12650
MLP	10.32(0.41)	3	1303	13.52(0.25)	3	22700
3BE	22.30(1.89)	3	6e+5	14.18(1.29)	5	2.2e+5

Table 1: Performance of RDRN and other methods for the shifting Gaussian and climate model datasets. L_2 denotes the L_2 loss, T is the optimal number of input time steps and N_p is the number of model parameters used. Lower loss values reflect better regression accuracies. The number in the parentheses is the standard error of the performance measures, over repeated runs.

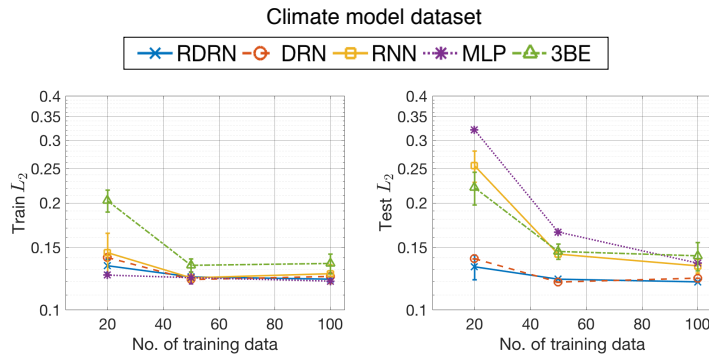


Figure 4: The train and test performance of all methods for the climate model dataset as number of training data varies. The accuracies of RDRN and DRN remain high as number of training data decreases, whereas RNN, MLP and 3BE saw more drastic decrease in accuracy. Errorbars are smaller than the size of the symbols when not shown. Best viewed in color.

3.3 Climate model

In the field of climate modeling, variability of climate measurements due to noise is an important factor to consider (Hasselmann, 1976). The next experiment is based on the work of Lin & Koshyk (1987), where they model the heat flux at the sea surface as a time-varying one-dimensional distribution. Specifically, the evolution of the heat flux over time obeys the stochastic Ornstein-Uhlenbeck (OU) process (Uhlenbeck & Ornstein, 1930) which describes how a unimodal distribution spreads and drifts over time. The heat flux’s diffusion and drift coefficients are determined from real data measurements obtained by Oort & Rasmusson (1971). We chose this dataset as the OU process is an important stochastic process with many real-world applications such as climate modeling (Hasselmann, 1976), neurobiology (Plesser & Tanaka, 1996) and commodity pricing (Schwartz & Smith, 2000). With this dataset, we test the ability of the regression methods to model unimodal Gaussian distributions spreading and drifting over time.

The OU process is described by a time-varying Gaussian distribution. With the long-term mean set at zero, the pdf has a mean of $\mu(t) = y \exp(-\theta t)$ and variance of $\sigma^2(t) = D(1 - e^{-2\theta t})/\theta$. t represents time, y is the initial point mass position, and D and θ are the diffusion and drift coefficients respectively. For the energy balance climate model, $D = 0.0013$, $\theta = 2.86$, and each unit of the nondimensional time corresponds to 55 days (Lin & Koshyk, 1987). At $t = 0$, the distribution is a delta-function at position y . To create a distribution sequence, we first sample $y \in [0.02, 0.09]$. For each sampled y , we generate 6 Gaussian distributions at $t_0 - 4\delta$, $t_0 - 3\delta$, ..., t_0 and $t_0 + 0.02$, with $\delta = 0.001$ and t_0 sampled uniformly from $[0.01, 0.05]$. The Gaussian distributions are truncated with support of $[-0.01, 0.1]$.

The regression task is as follows: Given the distributions at $t_0 - 4\delta$, $t_0 - 3\delta$, ..., t_0 , predict the distribution at $t_0 + 0.02$. With different sampled values for y and t_0 , we created 100 training and 1000 test data. The regression performance is measured by the L_2 loss. The regression results on the test set are shown in Table 1. RDRN’s and DRN’s regression accuracy are the best. This is followed by the neural network architectures MLP and RNN. It is noteworthy that RDRN and RNN,

CarEvolution (5 training data)				Stock (200 training data)				
	Test NLL	T	N_p		Test NLL (1 day)	Test NLL (10 days)	T	N_p
RDRN	3.9660(3e-4)	2	12313	RDRN	-469.47(2.43)	-459.14(0.01)	3	37
DRN	3.9663(2e-5)	2	28676	DRN	-473.93(0.02)	-458.08(0.01)	1	9
MLP	3.9702(6e-4)	2	1.2e+7	RNN	-467.37(1.33)	-457.96(0.20)	3	4210
3BE	3.9781(0.003)	2	1.2e+7	MLP	-471.00(0.04)	-457.08(0.98)	3	10300
EDD	4.0405	1	64	3BE	-464.22(0.16)	-379.43(11.8)	1	14000

(a)

(b)

Table 2: Performance of RDRN and other methods for the (a) CarEvolution and (b) stock dataset. NLL : negative log-likelihood, T : optimal number of input time steps, N_p : number of model parameters used. Lower loss values reflect better regression accuracies.

which explicitly capture time dependencies in the architecture, perform better with more time steps ($T=5$) compared to the feedforward models ($T=3$), which may suggest that the recurrent architecture captures the time dependencies in the data sequence better. In terms of model compactness, RDRN and DRN use 100 to 1000 times fewer model parameters compared to the other methods, owing to the compact distribution representation. To test the methods’ robustness to limited training data, we decreased the number of training data, as shown in Figure 4. The test performance of RDRN and DRN remains very good even at a low training size of 20, whereas the other methods of RNN, MLP and 3BE saw large decrease in performance. In addition, there is no significant difference in performance between RDRN and DRN for the varying training sizes.

3.4 CarEvolution data

For the next experiment, we use the CarEvolution dataset (Rematas et al., 2013) which was used by Lampert (2015) to evaluate EDD’s ability to track the distribution drift of image datasets. This is very useful for training classifiers where the data distribution changes over time. For this experiment, we include EDD as a benchmark method. The dataset consists of 1086 images of cars manufactured from the years 1972 to 2013. We split the data into intervals of 5 years (ie. 1970-1975, 1975-1980, ..., 2010-2015) where each interval has an average of 120 images. This gives 9 time intervals and for each interval, we create the data distribution from the DeCAF (fc6) features (Donahue et al., 2014) of the car images using kernel density estimation. The DeCAF features have 4096 dimensions. Performing accurate density estimation in very high dimensions is challenging due to the curse of dimensionality (Gu et al., 2013). Here we make the approximation that the DeCAF features are independent, such that the joint probability is a product of the individual dimension probabilities. In the shifting Gaussian and the climate model datasets, the distributions are unimodal and Gaussian. For this dataset, as shown in Fig. 8 in A.3, the distributions can be multimodal and non-Gaussians. Hence, we are evaluating the ability of the methods to track the time evolution of distributions which have more complex shapes than simple unimodal Gaussians.

The regression task is to predict the next time step distribution of features given the previous T time step distributions. We found $T=2$ to work best for all methods. The first 7 intervals were used for the train set while the last 3 intervals were used for the test set, giving 5 training and 1 test data. The regression performance is measured by the negative log-likelihood (NLL) of the test samples following Oliva et al. (2013), where lower negative log-likelihood is favorable. The regression results are shown in Table 2a. RDRN and DRN have the best test performance. RNN had difficulty in optimization possibly due to the high number of input dimensions, so the results are not presented. EDD has the fewest number of parameters as it assumes the dynamics of the distribution follows a linear mapping between the RKHS features of consecutive time steps (ie. $T=1$). However, as the results show, the EDD model may be too restrictive for this dataset. For this dataset, since the number of training data is very small, we do not conduct the experiments to see how the accuracy varies with the size of the training set.

3.5 Stock prediction

The next experiment is on stock price distribution prediction which has been studied extensively by Kou et al. (2018), with comparisons between DRN and several other methods. Here we perform

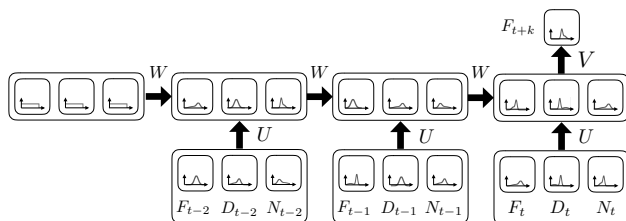


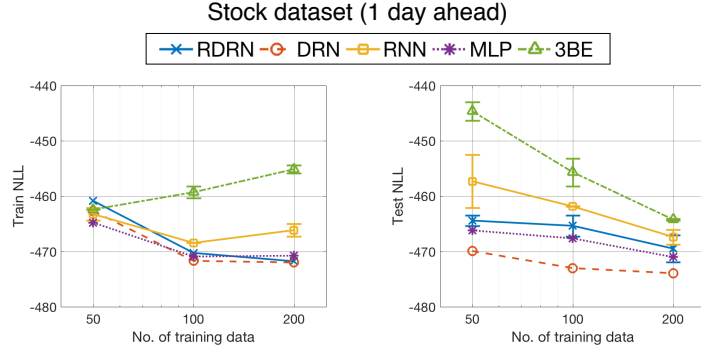
Figure 5: RDRN network for the stock dataset: past 3 days of distribution of returns of constituent companies in FTSE, DOW and Nikkei were used as inputs, to predict the future distribution of returns for constituent companies in FTSE. One layer of hidden states is used, with 3 nodes per hidden state.

a direct comparison with RDRN where we adopt a similar experimental setup. There have been studies showing that the movement of indices of stock markets in the world correlate with each other, providing a basis for predicting future stock returns (Hamao et al., 1990; Chong et al., 2008). Specifically, the previous day stock returns of the Nikkei and Dow Jones Industrial Average (Dow) are found to be good predictors of the FTSE return (Vega & Smolarski, 2012). Furthermore, predicting the entire distribution of stock returns has been found to be more useful for portfolio selection compared to just a single index value (Cenesizoglu & Timmermann, 2008). Hence, predicting future stock returns distributions has significant value in the real-world setting and here we test the methods’ abilities to perform such a task.

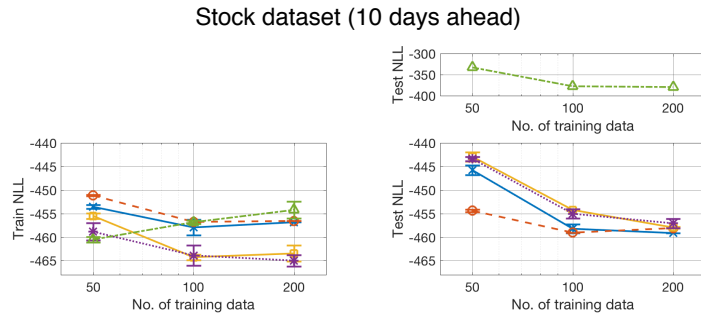
Following the setup in Kou et al. (2018), our regression task is as follows: given the past T days’ distribution of returns of constituent companies in FTSE, Dow and Nikkei, predict the distribution of returns for constituent companies in FTSE k days later. We used 5 years of daily returns from 2011 to 2015 and performed exponential window averaging on the price series following common practice (Murphy, 1999). We also used a sliding-window training scheme (Kaastra & Boyd, 1996) to account for changing market conditions (details are in A.4). Each distribution is obtained using kernel density estimation with the constituent companies’ returns as samples. In Fig. 9 in A.4, we show some samples of the distributions. The regression performance is measured by the negative log-likelihood of the test samples. The RDRN architecture used is shown in Figure 5, where the data input consists past 3 days of distribution returns and one layer of hidden states with 3 nodes per time step is used.

We tested on forward prediction of 1 and 10 days ahead. Table 2b shows the regression results for training size of 200. In addition, we decreased the number of training data to observe how robust the methods are when training data is limited. For 1 day ahead performance, DRN’s test accuracy consistently outperforms the other methods, followed by MLP then RDRN (see Figure 6a). Since for this experiment DRN uses only one previous day of input, this suggests that the 1 day ahead prediction task does not involve long time dependencies. When the training size decreases, the performance of DRN, RDRN and MLP remains about the same whereas RNN and 3BE have larger decrease in test accuracy.

Predicting 10 days ahead is a more challenging task which may benefit from having a longer history of stock movements. Table 2b shows that for a training size of 200, RDRN performs the best with 3 days of input history. For smaller training sizes, as shown in Figure 6b, DRN’s performance is better while the other methods saw larger decrease in test accuracy. 3BE’s accuracy is much lower than the other methods, hence its plot is shown on separate scales. This suggests that for a prediction task which involves longer time dependencies, having a recurrent architecture for DRN is beneficial when training size is sufficiently large. We further visualize the results by comparing the mean and variance of the predicted and the label distributions for training size of 200, as shown in Figure 7. Each point represents one test data. For 1 day ahead prediction, DRN’s mean and variance plots are the best, with the other methods showing larger errors. For the 10 days ahead prediction, as expected, the performance for all methods deteriorates. RDRN and DRN have the best regression performance as the points lie closest to the diagonal line, with the other methods showing larger errors, especially in the variance plots.



(a)



(b)

Figure 6: (a) Train and test negative log-likelihood (NLL) for the stock dataset for 1 day ahead prediction as the number of training data varies. DRN test performance surpasses the other methods even as the training size decreases. (b) The comparison of train and test NLL for the 10 days ahead prediction. 3BE’s test NLL is shown on a separate plot as its accuracy is much lower than the other methods. Errorbars are smaller than the size of the symbols when not shown. Best viewed in color.

4 Discussion

Neural network models work well by designing the architecture according to the data type. For regression on probability distributions, conventional neural networks, however, do not have suitable representations for distributions and are agnostic to the distribution nature of the input data. A recently proposed distribution regression network (DRN) (Kou et al., 2018) addresses this issue. DRN has a novel representation where each node encodes a distribution, showing improved accuracies compared to neural networks for the distribution-to-distribution regression task. However, the experiments in Kou et al. (2018) focused mainly on non-time series data and there is no systematic study on how DRN performs with limited annotated data. In this paper, we evaluate DRN for the new task of performing forward prediction on time sequences of probability distributions. Furthermore, to better model the time dependencies in a sequence of distributions, we propose our recurrent distribution regression network (RDRN) which extends DRN with a recurrent architecture.

Our experimental datasets feature a variety of tasks for forward prediction on sequences of probability distributions. We also conducted detailed studies on how the test performance varies with the size of training data, since for time series data, the amount of data may be limited given the seasonality of the data. On most datasets, RDRN and DRN achieve superior test performance than the neural network models and 3BE, and require 2 to 5 times fewer training data to achieve similar prediction accuracies. Because of the compact distribution representation, the models in RDRN and DRN use 4 to 300 times fewer model parameters than the neural network models. This highlights the importance of having suitable representations for distribution data. Between RDRN and DRN, their performances are largely similar. However, for the 10 days ahead stock prediction task, RDRN achieves better performance than DRN when there is sufficient training data, suggesting that the recurrent architecture is advantageous for prediction tasks involving longer time dependencies.

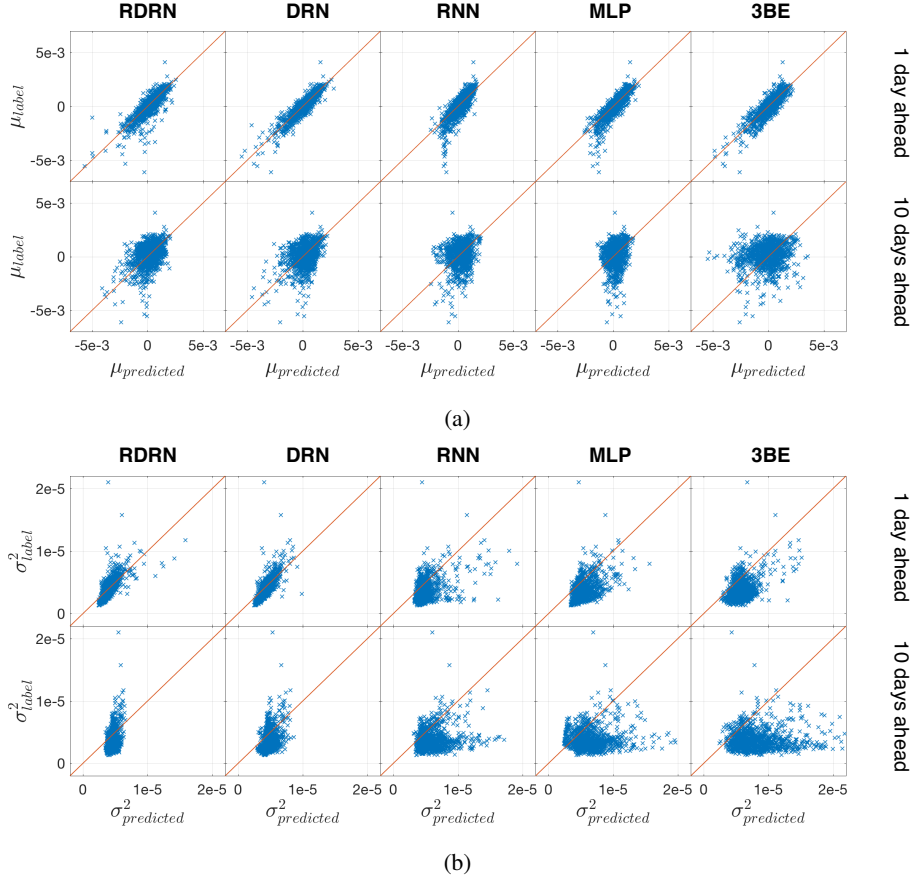


Figure 7: Comparison of the (a) mean and (b) variance of the label and predicted distributions for 1 and 10 days ahead stock prediction. The diagonal line represents a perfect fit.

Our studies show the strengths of the compact distribution representation in RDRN and DRN in distribution regression tasks that have applications in a wide range of fields. For future work, we look to extend to multivariate distributions, which will be useful in various applications such as modeling the 3D distribution of dark matter (Ravanbakhsh et al., 2016) and studying human populations through multi-dimensional census data (Flaxman et al., 2015).

A Experimental details

A.1 Shifting Gaussian

Table 3 shows the detailed network architectures used, for training size of 20. $q = 100$ was used for the discretization of the distributions.

A.2 Climate Model

Table 4 shows the detailed network architectures used, for training size of 100. $q = 100$ was used for the discretization of the distributions.

A.3 CarEvolution data

Table 5 shows the detailed network architectures used for the CarEvolution dataset, for training size of 5. $q = 100$ was used for the discretization of the distributions. Fig. 8 shows some samples of the distributions formed from the CarEvolution dataset. The distributions' shapes are much more varied than simple Gaussian distributions.

Comparison of models tuned for best validation set result (Shifting Gaussian dataset, 20 training data)

	Test $L_2(10^{-2})$	T	Model description	N_p	Cost function
RDRN	4.55(0.42)	3	T = 3, m = 5	59	JS divergence
DRN	4.90(0.46)	3	3 - 2x10 - 1	224	JS divergence
RNN	17.50(0.89)	3	T = 3, m = 10	2210	MSE
MLP	10.32(0.41)	3	300 - 1x3 - 100	1303	MSE
3BE	22.30(1.89)	3	30 basis functions, 20k RKS features	6e+5	L_2 loss

Table 3: Performance of RDRN and other methods for the shifting Gaussian dataset, with descriptions of the models. L_2 denotes the L_2 loss, T is the optimal number of input time steps and N_p is the number of model parameters used, MSE represents the mean squared error. A discretization of $q = 100$ is used for the distributions. For RDRN and RNN, m is the number of nodes in the hidden state of each time step. For DRN and MLP (feedforward networks), the architecture is denoted as such: Eg. 3 - 2x10 - 1: 3 input nodes, with 2 fully-connected hidden layers each with 10 nodes, and 1 output node.

Comparison of models tuned for best validation set result (Climate model dataset, 100 training data)

	Test $L_2(10^{-2})$	T	Model description	N_p	Cost function
RDRN	11.98(0.13)	5	T = 5, m = 5	59	JS divergence
DRN	12.27(0.34)	3	3 - 1x5 - 1	44	JS divergence
RNN	13.29(0.59)	5	T = 5, m = 50	12650	MSE
MLP	13.52(0.25)	3	300 - 2x50 - 100	22700	MSE
3BE	14.18(1.29)	5	11 basis functions, 20k RKS features	2.2e+5	L_2 loss

Table 4: Performance of RDRN and other methods for the climate model dataset, with descriptions of the models. L_2 denotes the L_2 loss, T is the optimal number of input time steps and N_p is the number of model parameters used, MSE represents the mean squared error. A discretization of $q = 100$ is used for the distributions. For RDRN and RNN, m is the number of nodes in the hidden state of each time step. For DRN and MLP (feedforward networks), the architecture is denoted as such: Eg. 3 - 2x10 - 1: 3 input nodes, with 2 fully-connected hidden layers each with 10 nodes, and 1 output node.

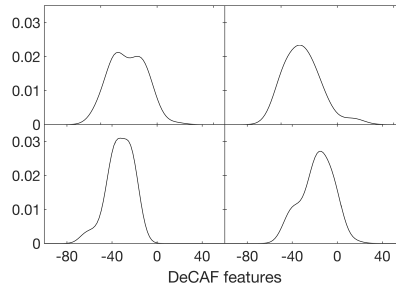


Figure 8: Samples of the DeCAF features (Donahue et al., 2014) distributions for the CarEvolution dataset, showing varied distribution shapes.

A.4 Stock prediction

The daily stock returns are the logarithmic returns. We used a sliding window scheme where a new window is created and the model retained after every 300 days (the size of the test set). For each window, the previous 500 and 100 days were used for training and validation sets respectively. Table 6 shows the detailed network architectures used. $q = 100$ was used for the discretization of the distributions. Fig. 9 shows some samples of the distributions formed from the stock dataset. The distributions' shapes much more varied than simple Gaussian distributions.

Comparison of models tuned for best validation set result (CarEvolution dataset, 5 training data)

	Test NLL	T	Model description	N_p	Cost function
RDRN	3.9660(3e-4)	2	$T = 2, m = 3$	12313	JS divergence
DRN	3.9663(2e-5)	2	(4096x2) - 1x1 - 4096	28676	JS divergence
MLP	3.9702(6e-4)	2	(4096x2x100) - 3x10 - (4096x100)	1.2e+7	MSE
3BE	3.9781(0.003)	2	15 basis functions, 200 RKS features	1.2e+7	L_2 loss
EDD	4.0405	1	8x8 kernel matrix for 8 training data	64	MSE

Table 5: Performance of RDRN and other methods for the CarEvolution dataset, with descriptions of the models. NLL denotes the negative log-likelihood, T is the optimal number of input time steps and N_p is the number of model parameters used, MSE represents the mean squared error. A discretization of $q = 100$ is used for the distributions. For RDRN and RNN, m is the number of nodes in the hidden state of each time step. For DRN and MLP (feedforward networks), the architecture is denoted as such: Eg. 3 - 2x10 - 1: 3 input nodes, with 2 fully-connected hidden layers each with 10 nodes, and 1 output node.

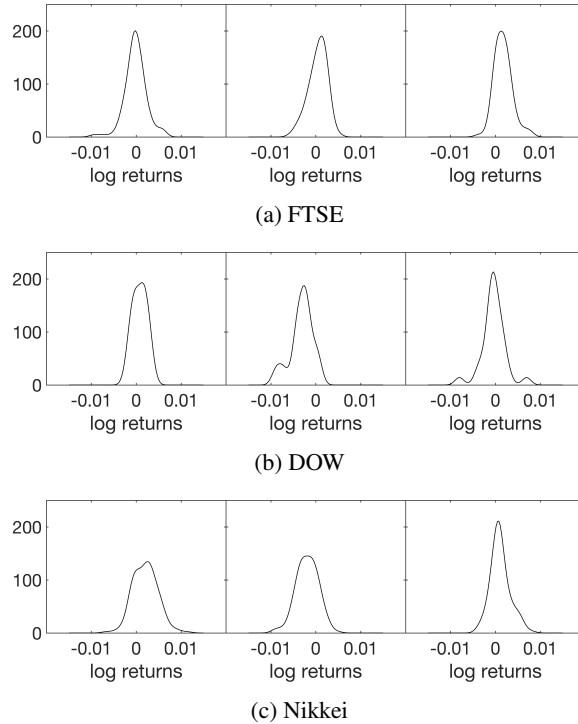


Figure 9: Samples of the data distributions formed from (a) FTSE, (b) DOW and (c) Nikkei constituent companies' log returns.

Comparison of models tuned for best validation set result (Stock dataset, 200 training data)

	Test NLL		T	Model description	N_p	Cost function
	1 day	10 days				
RDRN	-469.47(2.43)	-459.14(0.01)	3	$T = 3, m = 3$	37	JS divergence
DRN	-473.93(0.02)	-458.08(0.01)	1	No hidden layer	9	JS divergence
RNN	-467.37(1.33)	-457.96(0.20)	3	$T = 3, m = 10$	4210	MSE
MLP	-471.00(0.04)	-457.08(0.98)	3	(3x3x100) - 3x10 - 100	10300	MSE
3BE	-464.22(0.16)	-379.43(11.8)	1	14 basis functions, 1k RKS features	14000	L_2 loss

Table 6: Performance of RDRN and other methods for the stock dataset, with descriptions of the models. NLL denotes the negative log-likelihood, T is the optimal number of input time steps and N_p is the number of model parameters used, MSE represents the mean squared error. A discretization of $q = 100$ is used for the distributions. For RDRN and RNN, m is the number of nodes in the hidden state of each time step. For DRN and MLP (feedforward networks), the architecture is denoted as such: Eg. 3 - 2x10 - 1: 3 input nodes, with 2 fully-connected hidden layers each with 10 nodes, and 1 output node.

References

- Butler, Marguerite A and King, Aaron A. Phylogenetic comparative analysis: a modeling approach for adaptive evolution. *The American Naturalist*, 164(6):683–695, 2004.
- Cenesizoglu, Tolga and Timmermann, Allan G. Is the distribution of stock returns predictable? Available at SSRN 1107185, 2008.
- Chong, Terence Tai-Leung, Wong, Ying-Chiu, and Yan, Isabel Kit-Ming. International linkages of the Japanese stock market. *Japan and the World Economy*, 20(4):601–621, 2008.
- Donahue, Jeff, Jia, Yangqing, Vinyals, Oriol, Hoffman, Judy, Zhang, Ning, Tzeng, Eric, and Darrell, Trevor. Decaf: A deep convolutional activation feature for generic visual recognition. In *International conference on machine learning*, pp. 647–655, 2014.
- Flaxman, Seth R, Wang, Yu-Xiang, and Smola, Alexander J. Who supported obama in 2012?: Ecological inference through distribution regression. In *Proceedings of the 21th ACM SIGKDD International Conference on Knowledge Discovery and Data Mining*, pp. 289–298. ACM, 2015.
- Gu, Chong, Jeon, Yongho, and Lin, Yi. Nonparametric density estimation in high-dimensions. *Statistica Sinica*, pp. 1131–1153, 2013.
- Guérin, T, Prost, J, and Joanny, J-F. Bidirectional motion of motor assemblies and the weak-noise escape problem. *Physical Review E*, 84(4):041901, 2011.
- Hamao, Yasushi, Masulis, Ronald W, and Ng, Victor. Correlations in price changes and volatility across international stock markets. *Review of Financial studies*, 3(2):281–307, 1990.
- Hasselmann, Klaus. Stochastic climate models part i. theory. *tellus*, 28(6):473–485, 1976.
- Kaastra, Ieabeling and Boyd, Milton. Designing a neural network for forecasting financial and economic time series. *Neurocomputing*, 10(3):215–236, 1996.
- Katsura, Shigetoshi. Statistical mechanics of the anisotropic linear heisenberg model. *Physical Review*, 127(5):1508, 1962.
- Kou, Connie Khor Li, Lee, Hwee Kuan, and Ng, Teck Khim. A compact network learning model for distribution regression. *Neural Networks*, 2018. ISSN 0893-6080. doi: <https://doi.org/10.1016/j.neunet.2018.12.007>. URL <http://www.sciencedirect.com/science/article/pii/S0893608018303381>.
- Lampert, Christoph H. Predicting the future behavior of a time-varying probability distribution. In *Proceedings of the IEEE Conference on Computer Vision and Pattern Recognition*, pp. 942–950, 2015.
- Lee, Hwee Kuan, Schulthess, Thomas C, Landau, David P, Brown, Gregory, Pierce, John Philip, Gai, Z, Farnan, GA, and Shen, J. Monte Carlo simulations of interacting magnetic nanoparticles. *Journal of applied physics*, 91(10):6926–6928, 2002.
- Lee, Hwee Kuan, Landau, David P, and Schulthess, Thomas C. Monte Carlo simulations of phase transitions in Rb_2MnF_4 . *Journal of applied physics*, 93(10):7643–7645, 2003.
- Lin, Charles A and Koshyk, John N. A nonlinear stochastic low-order energy balance climate model. *Climate dynamics*, 2(2):101–115, 1987.
- Lin, Jianhua. Divergence measures based on the Shannon entropy. *IEEE Transactions on Information theory*, 37(1):145–151, 1991.
- Murphy, John J. Technical analysis of the futures markets: A comprehensive guide to trading methods and applications, New York Institute of Finance, 1999.
- Noble, PL and Wheatland, MS. Modeling the sunspot number distribution with a fokker-planck equation. *The Astrophysical Journal*, 732(1):5, 2011.

- Oliva, Junier, Neiswanger, William, Póczos, Barnabás, Xing, Eric, Trac, Hy, Ho, Shirley, and Schneider, Jeff. Fast function to function regression. In *Artificial Intelligence and Statistics*, pp. 717–725, 2015.
- Oliva, Junier B, Póczos, Barnabás, and Schneider, Jeff G. Distribution to distribution regression. In *ICML (3)*, pp. 1049–1057, 2013.
- Oliva, Junier B, Neiswanger, Willie, Póczos, Barnabás, Schneider, Jeff G, and Xing, Eric P. Fast distribution to real regression. In *AISTATS*, pp. 706–714, 2014.
- Oort, Abraham H and Rasmusson, Eugene M. *Atmospheric circulation statistics*, volume 5. US Government Printing Office, 1971.
- Palmer, Tim N. Predicting uncertainty in forecasts of weather and climate. *Reports on progress in Physics*, 63(2):71, 2000.
- Plesser, Hans E and Tanaka, Shigeru. Stochastic resonance in a model neuron with reset. *arXiv preprint physics/9611014*, 1996.
- Póczos, Barnabás, Singh, Aarti, Rinaldo, Alessandro, and Wasserman, Larry A. Distribution-free distribution regression. In *AISTATS*, pp. 507–515, 2013.
- Ravanbakhsh, Siamak, Oliva, Junier B, Fromenteau, Sebastian, Price, Layne, Ho, Shirley, Schneider, Jeff G, and Póczos, Barnabás. Estimating cosmological parameters from the dark matter distribution. In *ICML*, pp. 2407–2416, 2016.
- Rematas, Konstantinos, Fernando, Basura, Tommasi, Tatiana, and Tuytelaars, Tinne. Does evolution cause a domain shift? In *Proceedings VisDA 2013*, pp. 1–3, 2013.
- Risken, Hannes. Fokker-planck equation. In *The Fokker-Planck Equation*, pp. 63–95. Springer, 1996.
- Schwartz, Eduardo and Smith, James E. Short-term variations and long-term dynamics in commodity prices. *Management Science*, 46(7):893–911, 2000.
- Uhlenbeck, George E and Ornstein, Leonard S. On the theory of the Brownian motion. *Physical review*, 36(5):823, 1930.
- Vega, Jose G and Smolarski, Jan M. Forecasting FTSE Index using global stock markets. *International Journal of Economics and Finance*, 4(4):3, 2012.
- Wu, Fa-Yueh. The Potts model. *Reviews of modern physics*, 54(1):235, 1982.